Tasmanian School of Business and Economics
University of Tasmania

Discussion Paper Series N 2023-01

Global money supply and energy and non-energy commodity prices: A MS-TV-VAR approach

Stefano Grassi

University of Rome Tor Vergata, Italy

Francesco Ravazzolo

BI Norwegian Business School, Norway

Free University of Bozen-Bolzano, Italy

Joaquin Vespignani

University of Tasmania, Australia

Giorgio Vocalelli

University of Rome Tor Vergata, Italy

ISBN 978-1-922708-43-4

Global money supply and energy and non-energy commodity prices: A MS-TV-VAR approach

Stefano Grassi

Department of Economics and Finance, University of Rome Tor Vergata, Italy

Francesco Ravazzolo

Department of Data Science and Analytics, BI Norwegian Business School, Norway

Faculty of Economics, Free University of Bozen-Bolzano, Italy

Joaquin Vespignani

Tasmanian School of Business and Economics, University of Tasmania, Australia

Centre for Applied Macroeocnomics Analysis, ANU, Australia

Giorgio Vocalelli

Department of Economics and Finance, University of Rome Tor Vergata, Italy

September, 2022

Abstract

This paper shows that the impact of the global money supply is disproportionally high for energy than for non-energy commodities prices. An increase in the global money supply for energy commodity prices results mostly in demand-pull inflation. However, for non-energy commodity prices, an increase in global money supply results in demand-pull inflation and cost-push inflation, as energy is a critical input for non-energy commodities. We introduce a Markov Switching framework with time-varying transition probabilities to quantify this effect. This macro-econometric model accounts for periods when the global money supply growth is slow, moderate, and fast. We find that the response to global money supply shocks is higher for energy than for non-energy commodity prices. We also find heterogeneous responses for both energy and non-energy commodities across regimes.

Keywords: Global money supply; Energy and non-energy prices; Markov-Switching VAR.
JEL codes: C54; E31; F01; Q43.

1 Introduction

Understanding and quantifying the impact of global money supply on commodity prices is vital for monetary and fiscal policies. Commodity prices are important causes of macroeconomic fluctuations, such as inflation. Central banks increasingly coordinate global monetary policies in response to global financial and economic developments (see for example Kose et al., 2003, Taylor, 2013, Rey, 2015, and Miranda-Agrippino and Rey, 2020). The great recession (2008) and the great pandemic (2020) showed increasing coordination among central banks, resulting in an extraordinary increase in the global money supply. A frequent result in empirical macroeconomic studies is that increases in money supply lead to commodity prices overshooting (see for example the pioneer works of Frankel and Hardouvelis, 1983, and Frankel, 1984). In this paper, we look at this money-driven overshooting of commodity prices through the lenses of energy and non-energy commodity prices. We argue that an increase in the global money supply for energy commodity prices results solely in demand-pull inflation. In contrast, for non-energy commodity prices, an increase in global money supply results in demand-pull inflation and cost-push inflation since energy prices are a key input on all non-energy commodities (such as agriculture, raw material, fertilizers, precious metal, metals, and minerals). Consequently, the impact of the global money supply is expected to be larger for energy commodity prices than for non-energy commodity prices.

The literature on the relationship between the money supply and commodity prices dates back to the pioneering works of Frankel and Hardouvelis (1983), and Frankel (1984), who propose a theoretical model of *overshooting* in commodity markets. Since commodities trade in competitive and efficient financial markets, they will likely react to unanticipated movements of money growth also in the short run and more than proportionally. Figure 1 shows the monthly global money supply growth, together with the percentage log-returns of the commodity index at the same frequency, in the period from January 1996 to October 2020. It is worth noting that significant changes in the money supply may anticipate changes in the price of commodities. As Frankel and Hardouvelis (1983) and Frankel (1984) suggest, commodities seem to react more than proportionally to changes in the money supply. The most visible example was during the global financial crisis when the money

supply suffered a large contraction followed by a considerable drop in commodity prices. Similar patterns can be observed in the first months of 2010 and 2015, respectively.

Darius (2010) and Belke et al. (2010) find that global money supply shocks impact commodity prices. Ratti and Vespignani (2013) shows that monetary shocks in the BRIC countries have a more pronounced effect on commodity prices when compared to monetary shocks which come from the G3 economies. However, these studies are conducted in a linear framework, neglecting the possibility that the stance of the response may vary according to phases of economic activity. An exception is the work by Beckmann et al. (2014), who study the relationship between money supply and commodity prices, setting a Markov Switching (MS) Error Correction model in which the short-run dynamic is subject to regime shifts. Specifically, Beckmann et al. (2014) find evidence of two regimes that they identify as a regime in which commodity prices respond to disequilibria and a regime in which they do not. In contrast, we identify three different regimes underlying the money supply growth, which can be classified as periods of low, moderate, and excessive money supply growth.

We propose a Markov Switching framework with time-varying transition probabilities to estimate the impact of the global money supply on energy and non-energy commodity prices. Based on time-varying transition probabilities, our macro-econometric model distinguishes amongst three regimes; when global money supply growth is slow, moderate, and fast in response to different stages of the global financial cycle. To the best of our knowledge, this topic has not yet been studied within an MS framework with time-varying transition probabilities. This macro-econometric model is beneficial to understand the quantitative effect of global money supply on commodity prices at different stages of the global business cycle, providing critical information to policymakers and the private sector alike.

Our results suggest that energy commodity prices have the highest response (almost twice) in terms of magnitude. After one year, the impact of one standard deviation increase of an unanticipated global money supply shock is associated with a 20.3%(11.3%) increase in energy (non-energy) prices in the slow-money supply regime. For the moderate money-supply regime, the impact of one standard deviation increase of an unanticipated global money supply shock is associated with a 15.6%(7.4%) increase in energy (non-energy)

commodity prices. Finally, for the fast money-supply regime, the impact of one standard deviation increase of an unanticipated global money supply shock is associated with a 14.0%(6.0%) increase in energy (non-energy) commodity prices. Therefore, we present a plausible theoretical explanation of why the impact of unanticipated global money supply shocks is larger for energy than for non-energy commodity prices.

The remainder of this paper is organized as follows: in Section 2, we present the transmission mechanism of unanticipated global money supply shocks on energy and non-energy commodity prices. In Section 3, we introduce the MS-VAR model with time-varying transition probabilities and its relative estimation procedure. Section 4 describes the data. In Section 5, we report pieces of evidence of three regimes driving the money supply variable. In Section 6 we inspect the effect of an unanticipated shock of global money supply on commodity (energy and non-energy together) prices within each regime. In Section 7, the heterogenous responses of different commodity sectors to money supply shock are reported. Finally, in Section 8, the conclusions are drawn.

2 The transmission mechanism of an unanticipated global money supply shocks on energy and non-energy commodity prices

In this section, we introduce the mechanism which leads the impact of monetary policy on energy commodity prices to be more pronounced than on the prices of the non-energy commodity sector. First, it is useful to recall the transmission mechanism of the global money supply to commodity prices. In the same spirit of Frankel (1986), an unanticipated increase in the money supply leads to higher expected inflation. Since commodity prices are not sticky as other goods, the higher demand for commodities pushes up the prices. We show, however, that monetary policy has a heterogenous effect on energy and non-energy commodity prices/sectors.

Energy commodities are by far the largest commodity market in the world. For example, the crude oil market capitalization reached 1.41 trillion US dollars by 2021. Within the energy market, fossil fuel energy (oil, coal, and gas) combined accounts for around 85% of

the global energy consumption by 2021, according to Ritchie et al. (2022).

Energy commodities are a key input on all non-energy commodities (such as agriculture, raw material, fertilizers, precious metal, metals, and minerals).[1] For example, a notable case is agriculture commodities which are energy-intensive sectors as the required energy both directly in the form of fuel and electricity and indirectly through the use of energy-intensive inputs, such as fertilizers and pesticides, and transport. Similarly, precious metals, other metals, mineral extraction, and explorations also heavily rely on energy.

Consequently, an increase in the global money supply affects energy and non-energy commodity prices differently. More precisely, for an energy commodity prices, an increase in global money supply results in an increase in demand (demand-pull inflation), while for a non-energy commodity prices, an increase in global money supply results in both increases in demand (demand-pull inflation) but also a shift in supply (or cost-push inflation).

Figure 2 shows the different responses of energy and non-energy commodity prices to a global increase in the money supply. Figure 2(a) shows that when the global money supply increases, the demand for energy commodities shifts from D' to D''. The intersection of Q'' and P'' is the new equilibrium E''. The impact of an increase in global money supply on the non-energy commodity is illustrated in Figure 2(b). This figure shows that for non-energy commodities, an increase in global money supply led to a demand increase from D' to D'' and prices from P' to P''. However, because energy commodities are an input of production of non-energy commodities, S' shifts to the left to S'' reflecting a higher cost of production due to an increase in the cost of energy inputs. This shift in supply (and its respective price increase) reduces demand towards the new equilibrium E'''. Consequently, the final equilibrium for energy commodity prices is higher than for non-energy commodities.

3 The methodology

To assess the impact of an increase in global money supply on energy and non-energy commodity prices, we rely on a Markov Switching (MS) framework, see Hamilton (1989)

[1]Note that we use the definitions of the World Bank where energy commodities are oil, coal, and gas, and non-energy commodities include agriculture (beverages, food, grains, and other foods), the raw material (timber and other raw materials), fertilizers, precious metal, and metals and minerals. Please see: Commodity Markets (worldbank.org) for more details.

and Krolzig (1997), among others. MS models, allowing parameters to vary according to regimes, are powerful tools for modeling economic expansions and contractions. The MS literature is vast, and it proceeds in both directions: methodological and empirical. From a methodological perspective, the baseline MS time series model introduced by Hamilton (1989) has been extended to allow transition probabilities to vary over time, see Kaufmann (2015), Billio et al. (2016), and Bazzi et al. (2017). From an empirical perspective, although MS models have been employed to inspect the impact of an energy price shock on macroeconomic quantities, (Kilian, 2008, Hamilton, 2011), the literature overlooks the relationship between commodity variables and global money supply. This is the first attempt to study the impact of global money supply on energy and non-energy commodity prices within an MS framework with time-varying transition probabilities to the best of our knowledge.

3.1 The model

Let $\{\mathbf{y}_t\}_{t=1}^T$ denote a time series of K-variate economic observations. We assume that the probability distribution of $\{\mathbf{y}_t\}_{t=1}^T$ depends on the realizations of a latent discrete-time Markov chain process. The reduced form of the MS-VAR model reads as:

$$\mathbf{y}_t = \mathbf{a}(s_t) + \sum_{p=1}^{P} \mathbf{A}_p \mathbf{y}_{t-p} + \boldsymbol{\varepsilon}_t, \quad \boldsymbol{\varepsilon}_t \sim \mathcal{N}_K(\mathbf{0}, \boldsymbol{\Sigma}(s_t)), \tag{1}$$

where $\mathbf{a}(s_t)$ is a $K \times 1$ vector of intercepts with $s_t \in \{1, \ldots, M\}$ being the realization of a latent Markov chain process; $\mathbf{A}_p$ is a $K \times K$ matrix containing the autoregressive coefficients where p is the number of lags; $\mathcal{N}_K(\cdot, \cdot)$ denotes a K-variate Normal distribution; and $\boldsymbol{\Sigma}(s_t)$ is a $K \times K$ variance-covariance matrix. Following Krolzig et al. (2000), Billio et al. (2016), and Baştürk et al. (2014), we allow intercepts and the variance-covariance matrix to vary across regimes, and we restrict the autoregressive coefficients to be regime-independent. This assumption is motivated by Clements and Krolzig (1998), who show that the intercept mainly drives forecasting errors.

The stochastic properties of the latent Markov chain are described by the $(M \times M)$-

matrices of time-varying transition probabilities:

$$\mathbf{P}_t = \begin{bmatrix} p_{t,11} & p_{t,12} & \cdots & p_{t,1M} \\ p_{t,21} & p_{t,22} & \cdots & p_{t,2M} \\ \vdots & \vdots & \ddots & \vdots \\ p_{t,M1} & p_{t,M2} & \cdots & p_{t,MM} \end{bmatrix}, \tag{2}$$

with $p_{t,ij} = \mathbb{P}(s_t = i | s_{t-1} = j, \mathbf{V_t}, \boldsymbol{\theta}^{ij})$, $\forall i, j \in \{1, \ldots, M\}$ where $\mathbf{V}_t$ is a set of N exogenous variables and $\boldsymbol{\theta}^{ij}$ is a vector of parameters. Following Kaufmann (2015) and Billio et al. (2016), we model the time-varying transition probabilities using a Logit specification. Accordingly, a centered parametrization of the transition probabilities, in which exogenous variables drive the time variation of the transition probabilities, is assumed as follows:

$$p_{t,ij} = \frac{\exp\left((\mathbf{V}_t - \mathbf{c})' \boldsymbol{\theta}_1^{ij} + \theta_0^{ij}\right)}{\sum_{i=1}^{M} \exp\left((\mathbf{V}_t - \mathbf{c})' \boldsymbol{\theta}_1^{ij} + \theta_0^{ij}\right)}, \quad i, j = 1, \ldots, M, \tag{3}$$

where $\boldsymbol{\theta}^{ij} = \left(\theta_0^{ij}, \boldsymbol{\theta}_1^{ij'}\right)'$ and $\mathbf{c}$ is a vector of threshold parameters chosen to be the average of $\mathbf{V}_t$. For identification purposes, we let M be the reference regime. We assume that the vectors containing the parameters which drive the transition to the reference regime are null, i.e., $\boldsymbol{\theta}^{Mj} = \mathbf{0}$, $\forall j = 1, \ldots, M$.[2]

As standard in the MS literature, the model is re-parametrized using a partition of the set of regressors to simplify the estimation procedure's exposition. Particularly, $(1, \mathbf{y}_{t-1}', \ldots, \mathbf{y}_{t-p}')$ is divided into $M + 1$ subsets: $\overline{\mathbf{x}}_{0t} = \left(\mathbf{y}_{t-1}', \ldots, \mathbf{y}_{t-P}'\right)'$, a $(KP \times 1)$ vector of regime-independent coefficients, and $\overline{\mathbf{x}}_{it} = 1, i = 1, \ldots, M$, which are M vectors of one regime specific regressors. Finally, let $\boldsymbol{\xi}_t = (\xi_{1,t}, \ldots, \xi_{M,t})'$ be the vector of indicator functions which contains information regarding the realization of the latent Markov chain process, s_t, namely, $\xi_{i,t} = \mathbb{I}_{s_t = i}$, for $i = 1, \ldots, M$ and $t = 1, \ldots, T$, and rewrite the model in Equation (1) as follows:

$$\mathbf{y}_t = \mathbf{X}_{0t}\boldsymbol{\gamma}_0 + \sum_{i=1}^{M} \xi_{it}\mathbf{X}_{it}\boldsymbol{\gamma}_i + \boldsymbol{\varepsilon}_t, \quad \boldsymbol{\varepsilon}_t \sim \mathcal{N}_M\left(\mathbf{0}, \boldsymbol{\Sigma}\left(\boldsymbol{\xi}_t\right)\right), \tag{4}$$

[2]Please note that for $\boldsymbol{\theta}_1^{ij} = 0$, $\forall i, j = 1, \ldots, M$, the MS-VAR with time-varying transition probabilities reduces to the case with constant probabilities.

where: $\mathbf{X}_{0t} = (\mathbf{I}_K \otimes \overline{\mathbf{x}}'_{0t})$ and $\mathbf{X}_{it} = \mathbf{I}_K$ are, respectively, the regime-invariant and the regime-specific regressor matrices; $\boldsymbol{\gamma}_0 = \text{vec}\left((\mathbf{A}_1, \ldots, \mathbf{A}_P)'\right)'$ are the regime-invariant autoregressive parameters; $\boldsymbol{\Sigma}(\boldsymbol{\xi}_t) = \boldsymbol{\Sigma}(\boldsymbol{\xi}_t \otimes \mathbf{I}_K)$ where $\boldsymbol{\Sigma} = (\boldsymbol{\Sigma}_1, \ldots, \boldsymbol{\Sigma}_M)$ with $\boldsymbol{\Sigma}_i$ being the $K \times K$ regime specific variance-covariance matrix, and $\boldsymbol{\Sigma}(s_t) = \sum_{i=1}^{M} \boldsymbol{\Sigma}_i \xi_{it}$, see Equation (1); finally $\boldsymbol{\gamma}_i = \mathbf{a}_i$ is a $(K \times 1)$ vector containing the regime dependent equation intercepts, and $\mathbf{a}(s_t) = \sum_{i=1}^{M} \mathbf{a}_i \xi_{it}$, see Equation (1).

3.2 Bayesian inference

Given the generous parametrization of the MS-VAR model introduced in Section 3.1, the estimation strategies rely on Bayesian techniques. The possibility of restricting parameters with different prior beliefs makes Bayesian methods a powerful tool in macroeconomics to overcome overfitting issues, issues that may arise from many free parameters and the short time series, see Ciccarelli and Rebucci (2003).

We set up a Gibbs sampler algorithm to draw from the conditional posterior distributions, particularly we use the multi-move strategy to filter the latent regimes (Chib, 1996, Krolzig, 1997). The conditional posterior distribution from which parameters are sampled is retrieved by combining the complete data likelihood $p(\mathbf{y}, \boldsymbol{\Xi}|\boldsymbol{\phi})$, where $\boldsymbol{\phi} = (\boldsymbol{\gamma}, \boldsymbol{\Sigma}, \boldsymbol{\theta})$, with the prior distribution $p(\boldsymbol{\phi})$ as follows:

$$p(\boldsymbol{\phi}, \boldsymbol{\Xi}|\mathbf{y}) \propto p(\mathbf{y}, \boldsymbol{\Xi}|\boldsymbol{\phi}) p(\boldsymbol{\phi}), \tag{5}$$

where: $\mathbf{y} = \text{vec}(\mathbf{y}_1, \ldots, \mathbf{y}_T)$ is the $TK \times 1$ vector containing the observation; $\boldsymbol{\Xi} = (\boldsymbol{\xi}_1, \ldots, \boldsymbol{\xi}_T)$ is the $MT \times 1$ vector of indicator variables; $\boldsymbol{\gamma} = \text{vec}(\boldsymbol{\gamma}_1, \ldots, \boldsymbol{\gamma}_M)$ is a vector of the regressor coefficients; and $\boldsymbol{\theta}$ contains the parameters of the time-varying transition probabilities. Moreover:

$$p(\mathbf{y}, \boldsymbol{\Xi}|\boldsymbol{\phi}) = (2\pi)^{-\frac{TK}{2}} \prod_{t=1}^{T} |\boldsymbol{\Sigma}(s_t)|^{-\frac{1}{2}} \exp\left\{-\frac{1}{2}\mathbf{u}'_t \boldsymbol{\Sigma}(s_t)^{-1} \mathbf{u}_t\right\} \prod_{i=1}^{M}\prod_{j=1}^{M} p_{ij}^{\xi_{it}\xi_{jt-1}}, \tag{6}$$

and $\mathbf{u}_t = \mathbf{y}_t - ((1, \boldsymbol{\xi}_t') \otimes \mathbf{I}_K)\, \mathbf{X}_t \boldsymbol{\gamma}$, with:

$$\mathbf{X}_t = \begin{pmatrix} \mathbf{X}_{0t} & \mathbf{X}_{1t} & \dots & \mathbf{0} \\ \vdots & \vdots & \ddots & \vdots \\ \mathbf{X}_{0t} & \mathbf{0} & \dots & \mathbf{X}_{Mt} \end{pmatrix}. \tag{7}$$

The Gibbs sampler is divided into four steps. We first draw from the conditional posterior distribution of the VAR coefficients, $\boldsymbol{\gamma}_0$, independent of the hidden Markov chain. Secondly, we draw the state-dependent intercepts, $\boldsymbol{\gamma}_i$, together with the variance-covariance matrix, $\boldsymbol{\Sigma}_i$. Then, we draw from the conditional posterior distribution of the parameters of the transition probabilities, $\boldsymbol{\theta}^{ij}$. Finally, the fourth step draws the vector of latent states, $\boldsymbol{\Xi}$. Defining $\boldsymbol{\gamma}_{(-i)} = (\gamma_1, \dots, \gamma_{i-1}, \gamma_{i+1}, \dots, \gamma_M)$ and $\boldsymbol{\Sigma}_{(-i)} = (\boldsymbol{\Sigma}_1, \dots, \boldsymbol{\Sigma}_{i-1}, \boldsymbol{\Sigma}_{i+1}, \dots, \boldsymbol{\Sigma}_M)$ we can sketch here the estimation algorithm:

1) Draw $\boldsymbol{\gamma}_0$ from $f(\boldsymbol{\gamma}_0|\mathbf{y}, \boldsymbol{\Xi}, \boldsymbol{\gamma}_{(-i)}, \boldsymbol{\Sigma})$;

2) For $i = 1, \dots, M$:

   (a) draw $\boldsymbol{\gamma}_i$ from $f(\boldsymbol{\gamma_i}|\mathbf{y}, \boldsymbol{\Xi}, \boldsymbol{\gamma}_{(-i)}, \boldsymbol{\Sigma})$;

   (b) draw $\boldsymbol{\Sigma}_i^{-1}$ from $f\left(\boldsymbol{\Sigma}_i^{-1}|\mathbf{y}, \boldsymbol{\Xi}, \boldsymbol{\gamma}_i, \boldsymbol{\Sigma}_{(-i)}\right)$;

3) Draw $\boldsymbol{\theta}^{j1}, \dots, \boldsymbol{\theta}^{j(M-1)}$ from $f\left(\boldsymbol{\theta}^{j1}, \dots, \boldsymbol{\theta}^{j(M-1)}|\mathbf{y}, \boldsymbol{\Xi}, \boldsymbol{\gamma}_i\right)$;

4) Draw $\boldsymbol{\Xi}$ from $p\left(\boldsymbol{\Xi}|\mathbf{y}, \boldsymbol{\gamma}, \boldsymbol{\Sigma}, \boldsymbol{\theta}\right)$.

Details regarding the full posterior distributions in 1) to 3) are given in Appendix B, while the latent states are sampled using the multi-move sampling strategy (Chib, 1996; Krolzig, 1997). When dealing with mixture models in a Bayesian framework, the estimation must explicitly treat the invariance of the likelihood under relabelling of the mixture components to avoid the so-called label switching problem, described the first time by Redner and Walker (1984). The literature proposes different solutions to deal with it, see Frühwirth-Schnatter (2006) and references therein for an extensive discussion. To address the label switching, we constrain the intercept of the global money supply equation, α_i^{GL}, $\forall i = 1, \dots, M$, to be increasing across regimes, namely $\alpha_1^{GL} < \alpha_2^{GL} < \dots < \alpha_M^{GL}$. This

restriction has clear implications for the model and its interpretation. Indeed, imposing such a restriction implies that the conditional mean of the global money supply growth is lower in the first regime. Accordingly, it increases across regimes when moving to the Mth regime. This assumption is consistent with our interpretation of the regimes since our objective is to distinguish between periods of low money growth and periods of high money growth.

4 Data

Following Ratti and Vespignani (2015), we construct the global money supply variable using M2 denominated in US dollars of the seven largest economies worldwide[3] (China, EU, India, Japan, Russia, UK, and the US) as money supply measures. These data are sampled monthly, the highest frequency at which they are available, from January 1996 to October 2020, and Thomson Reuters provide them. Global money supply (GM2) is constructed as the sum of national monetary aggregates as follows:

$$GM2_t = \sum_{i=1}^{N} M2_{i,t}, \quad t = 1, \ldots, T \tag{8}$$

where $M2_{i,t}$ is the M2 money aggregate measure for country i at time t.

To assess the effect of an increase in money supply on commodity (energy and non-energy together) prices, we use the Global Price Index of All Commodities from FRED as a tracker of commodity prices (GCP). Data on short-term interest rates comes from the Federal Reserves Bank of Dallas, particularly from the Database of Global Economic Indicators. The global interest rate is calculated as the sum of the US policy rate and the World (excluding the US) short-term interest rate weighted by their respective share of global GDP as follows:

$$GIR_t = (1 - w_t^{US}) IR_t^{World} + w_t^{US} IR_t^{US}, \tag{9}$$

[3]The countries taken into account represent more than the 70% share of the world GDP according to the last published *World Bank data paper*.

where the weights w_t^{US} are constructed using the ratio between the quarterly data on GDP^{US} and GDP^{World}. The weights are assumed to be constant within the quarter, and the data are freely available at International Monetary Fund.

Global industrial production (GIP) and the global consumer price index (GCPI) drive the time-varying transition probabilities. Similar to the global interest rate variable, they are constructed using data from the Global Economic Indicators of the Federal Reserve Bank of Dallas by summing up their respective world and US variable weighted by the share of the global GDP. All endogenous variables are taken in monthly quarter-over-quarter (QoQ) percentage log differences. The vector of endogenous variables in Equation (1) is $\mathbf{y}_t' = 100(\Delta \ln(GM2_t), \Delta \ln(GIR_t), \Delta \ln(GCP_t))$, while the transition probabilities are driven by $\mathbf{V}_t' = (\Delta \ln(GIP_t,)\Delta \ln(GCPI_t))$.

Finally, we employ data from the World Bank to study the effect of a positive innovation in global money supply on prices of different sectors of the commodity markets. Specifically, we use the data on energy, non-energy, precious metals, agriculture, raw materials, and metals and minerals sectors stored in the "Pink Sheet" dataset of the World Bank.

5 Non-linearities in global money supply

In this section, we present the characteristics of the MS dynamic which drive global money supply. First, we determine the number of regimes that drive global money supply by comparing the goodness-of-fit of different model specifications. Secondly, by inspecting the kernel density estimates of the posterior draws of the regime-dependent parameters, we examine the features of the regime that the model detects. Then, we look at the smoothed probabilities produced by the MS-VAR. Finally, we check the contribution of the global economic indicators, i.e., global industrial production and consumer price index, to the probabilities of switching between regimes.

5.1 Number of regimes

To find evidence of an underlying non-unique regime driving the money supply growth at a global level, we estimate the VAR and the MS-VAR using different model specifications.

Then, the in-sample goodness-of-fit of each model is evaluated according to the Deviance Information Criterion (DIC), firstly introduced by Spiegelhalter et al. (2002). The DIC reads as follows:

$$\text{DIC} \doteq 2\left\{\ln \mathcal{L}\left(\bar{\boldsymbol{\phi}}|\mathbf{y}\right) - 2\mathbb{E}_{\boldsymbol{\phi}|\mathbf{y}}\left[\ln \mathcal{L}\left(\boldsymbol{\phi}|\mathbf{y}\right)\right]\right\}, \tag{10}$$

where $\mathbb{E}_{\boldsymbol{\phi}|\mathbf{y}}[\ln \mathcal{L}(\boldsymbol{\phi}|\mathbf{y})]$ is the expected value with respect to the joint posterior density, $\mathcal{L}(\boldsymbol{\phi}|\mathbf{y})$ is the likelihood, and $\bar{\boldsymbol{\phi}} = \mathbb{E}_{\boldsymbol{\phi}|\mathbf{y}}(\boldsymbol{\phi})$. Following Kaufmann and Frühwirth-Schnatter (2002) the likelihood function in Equation (10) can be rewritten as:

$$\mathcal{L}(\boldsymbol{\phi}|\mathbf{y}) = \prod_{t=1}^{T}\left[\sum_{i=1}^{M} p\left(\mathbf{y}_t|\boldsymbol{\phi}, s_t = i, \mathbf{y}^{t-1}\right)\mathbb{P}\left(s_t = i|\boldsymbol{\phi}, \mathbf{y}^{t-1}\right)\right], \tag{11}$$

where $p\left(\mathbf{y}_t|\boldsymbol{\phi}, s_t = i, \mathbf{y}^{t-1}\right)$ is the distribution of $\mathbf{y}_t$ conditioned to a single realization of the hidden Markov chain, and $\mathbb{P}\left(s_t = i|\boldsymbol{\phi}, \mathbf{y}^{t-1}\right)$ is the filtered probability. Similar to other information criteria, the DIC measures the balance between the goodness-of-fit and the model complexity. To identify the best number of latent regimes driving global money supply, we estimate the VAR and the MS-VAR with up to sixteen lags and three regimes. For each model under consideration, Table 4 shows the DIC with the corresponding confidence intervals.

Confidence intervals are constructed following Ardia (2009) who proposes to resample from the posterior estimates using the stationary block bootstrap of Politis and Romano (1994). This methodology allows estimating the uncertainty of the DIC without recomputing the model several times and, therefore, heavily reduces the computational burden. The optimal length of the blocks is chosen by applying the Politis and White (2004) methodology to each parameter using the resulting maximum value as the optimal length. The DIC reported in Table 4 supports the evidence of three regimes. Indeed, given the same number of lags, the MS(3)-VAR always outperforms the other specifications.

Regarding the order of the autoregressive coefficients, the DIC suggests that sixteen lags fit the data better but differences are not statistically significant. Therefore, to avoid possible overfitting problems which may arise using the DIC (Ando, 2007) and to find a more conclusive evidence on the number of lags, we also employ the predictive likelihood (PL), see Frühwirth-Schnatter (2006). While the DIC allows testing the in-sample goodness-

of-fit of each model, the PL serves to test the out-of-sample performance of the models. Specifically, we evaluate the PL for the MS(3)-VAR, with $p = 1, \ldots, 16$, and the one with the highest PL delivers the best out-of-sample goodness of fit. The PL suggests that the model with twelve lags has the best score in terms of predictive likelihood, see Table 2. Therefore, we choose the MS(3)-VAR with twelve lags.

5.2 Empirical identification of the regimes

In this section, we assess the features of the different regimes providing evidence of the regime identification. To do so, we inspect the kernel densities of the posterior draws of the regime-dependent parameters.

Figure 3 reports the kernel density estimates of the posterior draws of the regime-dependent intercepts. These posteriors encompass vital insights regarding the characteristics of commodity prices and the global interest rate in the different money supply regimes.

The first moments of the posterior densities of the intercepts of the global money supply equation are increasing across regimes; each regime represents a different state of the monetary cycle. The red shaded area refers to a period of low money growth; similarly, the blue and the green shaded areas refer to moderate and excessive credit growth regimes, respectively. As visible, both the supports of global money supply intercepts associated with the second and third regimes are positive and statistically different from zero. This result suggests that in both regimes global money supply tends to increase.

The regime-dependent intercepts of the commodity price equation are distinguishable across regimes suggesting that the conditional mean of the commodity price growth is substantially different depending on the phases of the monetary cycle. Specifically, the support of the intercept is negative and statistically different from zero in the first regime, namely, when money growth is slackening. This result points out that when the global money supply slowdowns also commodity prices tend to decrease. In the second regime, the commodity prices intercept is centered around zero, while it is positive and statistically different from zero during periods of excessive credit growth.

The intercept of the global interest rate associated with a contractionary period of credit growth is negative. This interest rate behavior is justified by the fact that in the

same period, commodity prices drop, and monetary authorities loosen the monetary policy to boost the economies. The intercepts' supports overlap in the second and third regimes, suggesting no clear difference across regimes.

Figure 4 shows the the other state-dependent parameter, i.e., the estimates of the variance-covariance matrices. The residual volatilities of the global money supply, global interest rate, and commodity prices are reported. As visible from the figure, there are similarities in the volatility behavior across variables. The first regime, associated with a slackening of money supply growth, is generally the most volatile period. In periods of money supply busts, usually resulting from a financial crisis, volatility increases because economic activity slowdowns and uncertainty grows. Conversely, the second and third regimes are much less volatile. In particular, the second is the least volatile period for money supply and nominal interest rate, while it is the third regime for commodity prices. Namely, during periods of high credit growth, commodity prices increase firmly.

5.3 Regime probabilities

This section provides the smoothed probabilities produced by the MS-VAR model. By inspecting these filtered probabilities, we can identify the periods associated with each regime. In this respect, the upper panel in Figure 5 shows the filtered probabilities produced by the model; particularly, the red shaded area, the blue one, and the green part refer to the first, second, and third regime, respectively.

As visible, the first part of the sample is characterized by periods of booms and busts in global money supply growth; conversely, from 2003 onwards, the global money supply growth witnessed a steadily increasing interrupted by some periods of money contraction during financial distresses. The rise in the level of money that began in 2003 is also recognized as the beginning of the global liquidity cycle, see Kokeyne et al. (2010), which accelerated from 2009 onwards when policymakers worldwide began to adopt liquidity easing measures to respond to the financial crisis.

Looking at the upper panel of Figure 5, it is worth noting that before the Great Recession in 2009, it was a period of increasing money supply that accelerated just before the crisis, and a regime of poor credit growth then followed it. A similar path can be observed

in the early 2000s, namely, during the dot-com bubble, and during the period of the covid-19 pandemic. As shown by Meller and Metiu (2017), Schularick and Taylor (2012), and Gourinchas and Obstfeld (2012), recession periods are often preceded by money booms, and they are generally accompanied by a drying up of money in circulation.

From 2010 to 2020, monetary aggregates have maintained sustained growth. This was the period when western economies implemented unconventional monetary policies and increased money in circulation. UE and US were the most active in quantitative easing, injecting vast amounts of money into the system.

In the first two quarters of 2020, as the lockdowns kicked in as a response to the covid-19 pandemic, is a higher probability of being in a regime of poor money growth. In the aftermath of the recession, policymakers worldwide implement expansionary monetary measures to support the economies, leading the world to an excessive money supply growth regime.

Finally, in the lower panel of Figure 5, the commodity price index (black dotted line) is shown, together with the filtered states (red line). In particular, the red line takes the value 5 (-5) when it is evidence of being in the third (first) regime and a value equal to zero when it is evidence of being in the second regime. As visible, commodities behave accordingly to money supply growth regimes. In particular, they rise when money growth accelerates and decrease accordingly. As shown in the figure, commodities prices crashed after the dot-com bubble, the Great Financial crisis, and the covid-19 recession.

5.4 Time-varying transition probabilities

One important novelty of our approach when studying the relationship between money and commodities is that the MS-VAR we propose allows transition probabilities to vary over time. In particular, the dynamic of the transition probabilities is parametrized á la Kaufmann (2015), and we assume that global indicators of economic activity drive the matrix of transition probabilities. Namely, the probability of switching between global credit regimes depends on global industrial production and the global consumer price index. Table 3 shows the posterior means of the parameters associated with each variable, together with the 90% confidence interval (in parenthesis).

First, it is worth highlighting that most coefficients are statistically significant, meaning that both variables have a non-trivial effect on the probability of switching across regimes. Moreover, global industrial production and the global consumer price index play an analogous role in the probability of switching between regimes.

The first row of Table 3 shows the coefficient associated with the global industrial production and global consumer price index on the probability of remaining in a low money supply growth regime or moving from the first regime to a regime of moderate global money supply increase. As visible, an increase in the global consumer price index and global industrial production increases the probability of remaining in the first regime. In contrast, it reduces the likelihood of going to the second regime. Similarly, $\theta_1^{j2}, j = 1, 2$, and $\theta_2^{j2}, j = 1, 2$, suggest that when global industrial production and consumer price index boost, the probability of passing from the second regime to the first regime increases, while it reduces the likelihood of remaining in the second one. When the global economy is in a period of excessive credit growth, i.e., in the third regime, increasing the global consumer price index and global industrial production leads to higher probabilities of returning to the first or the second regime.

6 Structural form

To investigate how an unanticipated monetary shock propagates to commodity prices, and vice-versa, the reduced model in Equation (1) needs to be transformed into a structural form. Let us consider the following equation:

$$\mathbf{y}_t' \mathbf{B}_0(s_t) = \boldsymbol{x}_t' \mathbf{B}_+(s_t) + \boldsymbol{u}_t', \tag{12}$$

where: $\boldsymbol{x}_t = (1, \mathbf{y}_{t-1}, \ldots, \mathbf{y}_{t-P})$. The parameters $\mathbf{A}(s_t) = (\mathbf{a}(s_t), \mathbf{A}_1, \ldots, \mathbf{A}_p)$ are estimated in the reduced form, $\mathbf{A}(s_t)' = \mathbf{B}_+(s_t)\mathbf{B}_0(s_t)^{-1}$, $\boldsymbol{\varepsilon}_t = \mathbf{B}_0(s_t)^{-1}\boldsymbol{u}_t$, and $\boldsymbol{\Sigma}(s_t) = (\mathbf{B}_0(s_t)\mathbf{B}_0(s_t)')^{-1}$. By imposing sufficient conditions on $(\mathbf{B}_0(s_t)\mathbf{B}_0(s_t)')$ the structural form is identified. Nevertheless, the reduced form parameters do not uniquely identify structural parameters and shocks across equations. Therefore it is impossible to distinguish regime shift from one structural equation to another, see Sims and Zha (2006) for an extensive

discussion.

We use a Cholesky ordering to identify the shocks. The commodity variable is assumed to respond contemporaneously to a global money supply shock and a global interest rate shock. In contrast, the global money supply responds to interest rates and commodity prices with a one-month lag.

Figure 6 shows the cumulated impulses response functions (IRFs) of commodity prices and interest rates to a one standard deviation increase of an unanticipated global money supply shock in each regime. As seen in the chart, an exogenous increase in global money supply leads to a temporary rise in commodity prices in each regime. In the first regime, when monetary growth is low, commodity prices are likely to react more than in the other regimes to an unanticipated shock in the money supply. In the long run, the shock is absorbed within 14 months when money growth is in one of the two increasing regimes, while it is absorbed in about twelve months when money growth is in the first regime.

Conversely, impulse responses of interest rate to a one standard deviation increase of an unanticipated global money supply shock are not statistically significant in any regime. At a global level, there is no clear evidence of what should be the effect of an increase in global money supply on the global interest rate. Following the reasoning of Ratti and Vespignani (2015), who find similar results, at the worldwide level, no unique central bank rules interest rates.

Figure 7 showcases the cumulated responses of money growth and commodity prices to a one standard deviation increase of an unanticipated global interest rate shock. As visible, global monetary aggregates do not respond to the rise in the global interest rate. Commodity prices positively react to an unexpected increase in nominal interest rates in the first regime. In contrast, when the worldwide monetary aggregate increases, it does not respond to commodity prices.

Figure 8 reports the cumulated impulse response functions of global money supply and global interest rate to a one standard deviation increase of an unanticipated commodity price shock. A one standard deviation increase in commodity price leads to a rise in nominal interest rates worldwide. This is in line with previous research. When commodity prices increase, monetary authority increases the nominal interest rate to offset the chance of an

increase in inflation. The response of global money supply to a commodity prices shock is unclear and not statistically significant.

7 The heterogenous effect of global money supply on energy and non-energy commodity prices

In this section, we focus our attention on the responses of prices of different commodity prices to unanticipated shocks in the global money supply. Particularly, we are interested in studying the heterogenous effect of an increase in global money supply to energy and non-energy commodity prices.

To do so, we use the same model as in Equation (4), but rather than the variable $\Delta \ln(GCP_t)$, we employ the percentage log changes of index prices that refer to different sectors of the commodity markets. Accordingly, we employ six indexes that track the evolution of the following commodity prices: energy and non-energy, and moreover, we inspect precious metals, agriculture, raw materials, and metals and minerals prices within the non-energy commodity.

We report in Figure 9 the cumulated IRFs of these prices to a one standard deviation increase of an unanticipated global money supply shock within each regime, while we show the value of impulse response functions, together with respective confidence bandwidths, in Appendix C.

Each row in Figure 9 represents one regime. Accordingly, in the upper panel are reported median responses of individual commodity prices to a positive shock in global money supply in the first regime, in the middle panel are reported responses in the second regime, and, similarly, in the lower panel, responses in the third regime are showcased.

Consistently with previous results, all prices positively react to a one standard deviation increase of an unanticipated global money supply shock. Figure 9 shows that after one year, the impact of one standard deviation increase in the global money supply is associated with a 20.3% (11.3%) increase in energy (non-energy) commodity prices in the slow money-supply regime. For the moderate money-supply regime, the impact of one standard deviation increase in the global money supply is associated with a 15.6% (7.4%) increase

in energy (non-energy) commodity prices. Finally, for the fast money-supply regime, the impact of one standard deviation increase in the global money supply is associated with a 14.0% (6.0%) increase in energy (non-energy) commodity prices.

By further inspecting commodities in the non-energy sector, we can see that, after one year, a one standard deviation increase of an unanticipated global money supply shock in the slow-money supply regime leads to a rise of 6.1%, 8.7%, 8.7%, and 9.1% for prices of precious metals, agriculture, raw materials, and metals and minerals, respectively. When the one standard deviation increase of an unanticipated global money supply shock is in the moderate money-supply regime, after one year, prices of precious metals, agriculture, raw materials, and metals and minerals increase by 6.4%, 6.7%, 5.4%, and 9.1%. Finally, in the fast money-supply regime, as a consequence of a one standard deviation increase of an unanticipated global money supply shock, prices of precious metals, agriculture, raw materials, and metals and minerals increase by 5.6%, 5.9%, 6.9%, and 7.8%.

When comparing the magnitude of the shocks, it is worth noting that the energy commodity prices tends to respond more pronouncedly to a positive rise in global money supply compared to the non-energy commodity prices in each regime. Particularly, the response magnitude is twice as large as the non-energy prices. As shown in Section 2, given that energy commodities are a key input of non-energy commodities, an increase in money supply leads to heterogenous effects on energy and non-energy commodity prices. Indeed, increasing money in circulation increases commodity demand, raising prices. However, the higher costs faced by non-energy producers reduce the supply of such commodities. As a result, the shift in supply, and its respective price increase, reduces demand toward a new equilibrium with lower prices.

8 Conclusions

This paper examines the impact of unanticipated global money supply shocks on energy and non-energy commodity prices using a Markov Switching framework with time-varying transition probabilities with monthly data from January 1996 to October 2020. We assess these unanticipated shocks in three different regimes to capture different stages of the global monetary cycle, which can be interpreted as periods when the global money supply is: slow,

moderate, and fast.

We present a plausible theoretical explanation of why the impact of unanticipated global money supply shocks is larger for energy than for non-energy commodity prices. We argue that an increase in the global money supply for energy commodities results solely in demand-pull inflation. However, for non-energy commodities, an increase in global money supply results in demand-pull inflation and cost-push inflation since energy commodities are a key input of all non-energy commodities.

Our results indicate that the impact of one standard deviation increase in the global money supply is associated with a 20.3% (11.3%) increase in energy (non-energy) commodity prices in the slow-money supply regime after 12 months. For the moderate money-supply regime, the impact of one standard deviation increase in the global money supply is associated with a 15.6% (7.4%) increase in energy (non-energy) commodity prices. Finally, for the fast money-supply regime, the impact of one standard deviation increase in the global money supply is associated with a 14.0% (6.0%) increase in energy (non-energy) commodity prices. These heterogeneous results across commodities are very informative to central banks, international organizations, and macroeconomic forecasters, who aim to understand the relationship between monetary cycles and commodity prices.

References

Ando, T. (2007). Bayesian Predictive Information Criterion for the Evaluation of Hierarchical Bayesian and Empirical Bayes Models. *Biometrika*, 94:443–458.

Ardia, D. (2009). Bayesian Estimation of a Markov-Switching Threshold Asymmetric GARCH Model with Student-t Innovations. *The Econometrics Journal*, 12:105–126.

Baştürk, N., Çakmakli, C., Ceyhan, S. P., and Van Dijk, H. K. (2014). Posterior-Predictive Evidence on US Inflation using Extended new Keynesian Phillips Curve Models with Non-Filtered Data. *Journal of Applied Econometrics*, 29:1164–1182.

Bazzi, M., Blasques, F., Koopman, S. J., and Lucas, A. (2017). Time-Varying Transition Probabilities for Markov Regime Switching Models. *Journal of Time Series Analysis*, 38:458–478.

Beckmann, J., Belke, A., and Czudaj, R. (2014). Does Global Liquidity Drive Commodity Prices? *Journal of Banking & Finance*, 48:224–234.

Belke, A., Orth, W., and Setzer, R. (2010). Liquidity and the Dynamic Pattern of Asset Price Adjustment: A Global View. *Journal of Banking & Finance*, 34:1933–1945.

Billio, M., Casarin, R., Ravazzolo, F., and Van Dijk, H. K. (2016). Interconnections Between Eurozone and US Booms and Busts Using a Bayesian Panel Markov-Switching VAR Model. *Journal of Applied Econometrics*, 31:1352–1370.

Chib, S. (1996). Calculating Posterior Distributions and Modal Estimates in Markov Mixture Models. *Journal of Econometrics*, 75:79–97.

Ciccarelli, M. M. and Rebucci, M. A. (2003). Bayesian VARs: A Survey of the Recent Literature with an Application to the European Monetary System. Technical report.

Clements, M. P. and Krolzig, H.-M. (1998). A Comparison of the Forecast Performance of Markov-Switching and Threshold Autoregressive Models of US GNP. *The Econometrics Journal*, 1:47–75.

Darius, M. R. (2010). *Can Global Liquidity Forecast Asset Prices?* International Monetary Fund.

Frankel, J. A. (1984). Commodity Prices and Money: Lessons from International Finance. *American Journal of Agricultural Economics*, 66:560–566.

Frankel, J. A. (1986). Expectations and Commodity Price Dynamics: The Overshooting Model. *American Journal of Agricultural Economics*, 68:344–348.

Frankel, J. A. and Hardouvelis, G. A. (1983). Commodity Prices, Overshooting, Money Surprises, and Fed Credibility. Technical report, National Bureau of Economic Research.

Frühwirth-Schnatter, S. (2006). *Finite Mixture and Markov Switching Models*. Springer Science & Business Media.

Gourinchas, P.-O. and Obstfeld, M. (2012). Stories of the Twentieth Century for the Twenty-First. *American Economic Journal: Macroeconomics*, 4:226–65.

Hamilton, J. D. (1989). A New Approach to the Economic Analysis of Nonstationary Time Series and the Business Cycle. *Econometrica: Journal of the econometric society*, pages 357–384.

Hamilton, J. D. (2011). Nonlinearities and the Macroeconomic Effects of Oil Prices. *Macroeconomic Dynamics*, 15:364–378.

Kaufmann, S. (2015). K-state Switching Models with Time-Varying Transition Distributions - Does Loan Growth Signal Stronger Effects of Variables on Inflation? *Journal of Econometrics*, 187:82–94.

Kaufmann, S. and Frühwirth-Schnatter, S. (2002). Bayesian Analysis of Switching ARCH Models. *Journal of Time Series Analysis*, 23:425–458.

Kilian, L. (2008). The Economic Effects of Energy Price Shocks. *Journal of economic literature*, 46:871–909.

Kokeyne, A., Nowak, S., Psalida, E., and Sun, T. (2010). Global Liquidity Expansion: Effects on Receiving Economies and Policy Response Options. *IMF Global Financial Stability Report*.

Kose, M. A., Prasad, E. S., and Terrones, M. E. (2003). How Does Globalization Affect the Synchronization of Business Cycles? *American Economic Review*, 93:57–62.

Krolzig, H.-M. (1997). *Markov-switching Vector Autoregressions: Modelling, Statistical Inference, and Application to Business Cycle Analysis*. Lecture Notes in Economics and Mathematical Systems. New York/Berlin/Heidelberg: Springer.

Krolzig, H.-M. et al. (2000). *Predicting Markov-Switching Vector Autoregressive Processes*. Nuffield College Oxford.

Meller, B. and Metiu, N. (2017). The Synchronization of Credit Cycles. *Journal of Banking & Finance*, 82:98–111.

Miranda-Agrippino, S. and Rey, H. (2020). US Monetary Policy and the Global Financial Cycle. *The Review of Economic Studies*, 87:2754–2776.

Politis, D. N. and Romano, J. P. (1994). The Stationary Bootstrap. *Journal of the American Statistical association*, 89:1303–1313.

Politis, D. N. and White, H. (2004). Automatic Block-Length Selection for the Dependent Bootstrap. *Econometric reviews*, 23:53–70.

Ratti, R. A. and Vespignani, J. L. (2013). Why Are Crude Oil Prices High When Global Activity is Weak? *Economics Letters*, 121:133–136.

Ratti, R. A. and Vespignani, J. L. (2015). Commodity Prices and BRIC and G3 Liquidity: A SFAVEC Approach. *Journal of Banking & Finance*, 53:18–33.

Redner, R. A. and Walker, H. F. (1984). Mixture Densities, Maximum Likelihood and the EM Algorithm. *SIAM Review*, 26:195–239.

Rey, H. (2015). Dilemma Not Trilemma: the Global Financial Cycle and Monetary Policy Independence. Technical report, National Bureau of Economic Research.

Ritchie, H., Roser, M., and Rosado, P. (2022). Energy. *Our World in Data*. https://ourworldindata.org/energy.

Schularick, M. and Taylor, A. M. (2012). Credit Booms Gone Bust: Monetary Policy,Leverage Cycles, and Financial Crises, 1870-2008. *American Economic Review*, 102:1029–61.

Sims, C. A. and Zha, T. (2006). Were there Regime Switches in US Monetary Policy? *American Economic Review*, 96:54–81.

Spiegelhalter, D. J., Best, N. G., Carlin, B. P., and Van Der Linde, A. (2002). Bayesian Measures of Model Complexity and Fit. *Journal of the royal statistical society: Series b (statistical methodology)*, 64:583–639.

Taylor, J. B. (2013). International Monetary Policy Coordination: Past, Present and Future.

Lag	VAR			MS(2)-VAR			MS(3)-VAR		
	5%	DIC	95%	5%	DIC	95%	5%	DIC	95%
2	4639.1	4639.5	4639.8	4371.3	4371.8	4372.5	4330.7	4338.3	4342.9
4	4416.7	4462.2	4462.8	4206.5	4207.2	4207.9	4158.3	4166.1	4178.7
8	4348.3	4348.8	4394.4	4097.0	4097.9	4098.8	4067.0	4070.5	4074.0
12	4275.2	4275.8	4276.4	4026.0	4027.1	4028.3	3982.1	3984.7	3987.7
14	4275.2	4275.8	4276.4	3988.7	3990.3	3991.7	3943.6	3945.5	3948.0
16	4275.2	4275.8	4276.4	3964.3	3966.3	3967.7	3924.3	3927.4	3929.3

Table 1: The Table reports the estimated DIC computed for the Vector Autoregressive Model (VAR), the Markov Switching VAR with two states (MS(2)-VAR), and the Markov Switching VAR with three states (MS(3)-VAR). The Table also reports the 5% and the 95% confidence interval constructed using the block-bootstrap of Politis and Romano (1994). The DIC suggests twelve lags for the VAR for all the models.

Model	2	4	8	12	14	16
MS(3)-VAR	-2288.6	-2331.0	-2384.0	-2098.5	-2146.2	-2243.4

Table 2: The Table reports the estimated predictive likelihood (PL) computed for the Markov Switching VAR with three states (MS(3)-VAR). The PL suggests twelve lags as the best specification.

Time-varying transition probabilities					
	$\Delta Log(GIP_t)$			$\Delta Log(GCPI_t)$	
	j=1	*j=2*		*j=1*	*j=2*
θ_1^{j1}	0.411	-0.305	θ_2^{j1}	0.383	-0.303
	(0.115, 0.706)	(-0.577, -0.034)		(0.094, 0.686)	(-0.609, -0.002)
θ_1^{j2}	0.407	-0.300	θ_2^{j2}	0.408	-0.298
	(0.107, 0.693)	(-0.585, 0.016)		(0.112, 0.720)	(-0.587, -0.003)
θ_1^{j3}	0.412	0.407	θ_2^{j3}	0.395	0.390
	(0.107, 0.699)	(0.136, 0.694)		(0.111, 0.680)	(0.106, 0.659)

Table 3: Posterior mean and 90% credible interval (in parenthesis) for the coefficients of the variables global industrial production ($\Delta Log(GIP_t)$) and global consumer price index ($\Delta Log(GCPI_t)$) which enter in the dynamic of the transition probabilities.

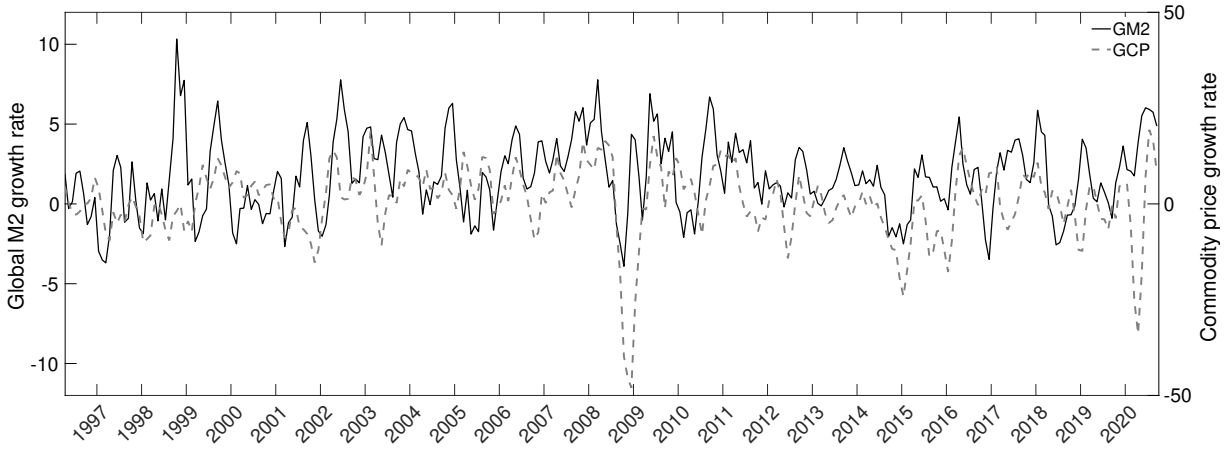

Figure 1: The figure plots the monthly growth rate of global M2 (GM2) with the scale on the left part (black line) and the global commodity index (GCP) with the scale on the right part (grey dashed line), from January 1996 to October 2020.

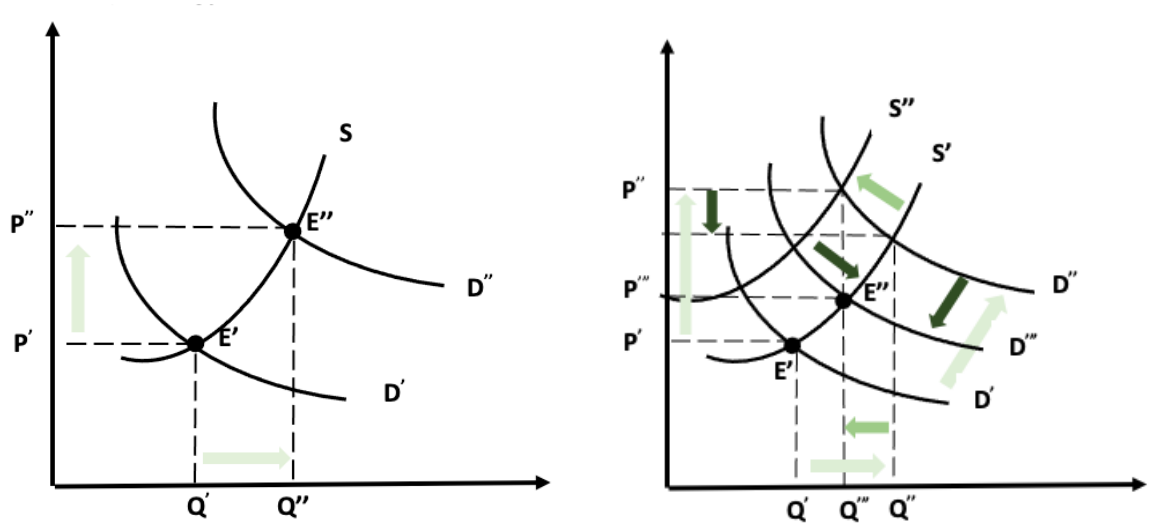

(a) Energy (b) Non-energy

Figure 2: The X-axis and Y-axis represent the measures of the quantity (Q) produced and prices (P), respectively. Curve S represents the supply and curve D represents the demand. Panel (a): It shows that energy demand and prices increase in response to an increase in the global money supply. Panel (b): It shows that non-energy demand and prices increase in response to an increase in the global money supply. However, because energy commodities are input on the production of non-energy commodities, the supply shifts to the left. Furthermore, this shift in supply reduces demand towards the new equilibrium E'''.

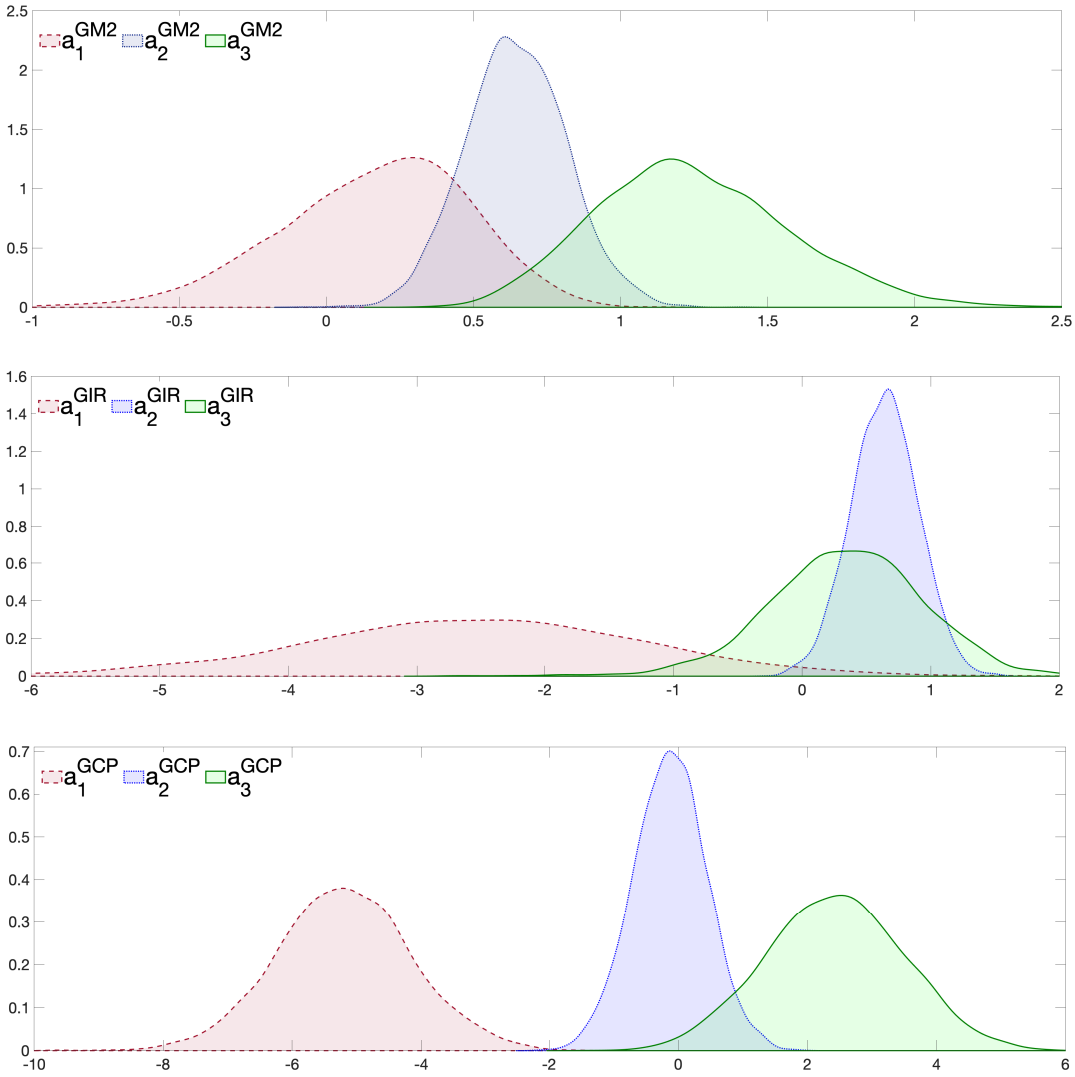

Figure 3: Upper panel: a_1^{GM2}, a_2^{GM2}, *and* a_3^{GM2} *are respectively kernel density estimates of the posterior draws of the regime-dependent intercept of the global money supply equation in the first (red shaded area with dashed line), second (blue shaded area with dotted line), and third (green shaded area with continuous line) regimes. Middle panel:* a_1^{GIR}, a_2^{GIR}, *and* a_3^{GIR} *are respectively kernel density estimates of the posterior draws of the regime-dependent intercept of the global interest rate equation in the first (red shaded area with dashed line), second (blue shaded area with dotted line), and third (green shaded area with continuous line) regimes. Lower panel:* a_1^{GCP}, a_2^{GCP}, *and* a_3^{GCP} *are respectively kernel density estimates of the posterior draws of the regime-dependent intercept of the commodity price equation in the first (red shaded area with dashed line), second (blue shaded area with dotted line), and third (green shaded area with continuous line) regimes.*

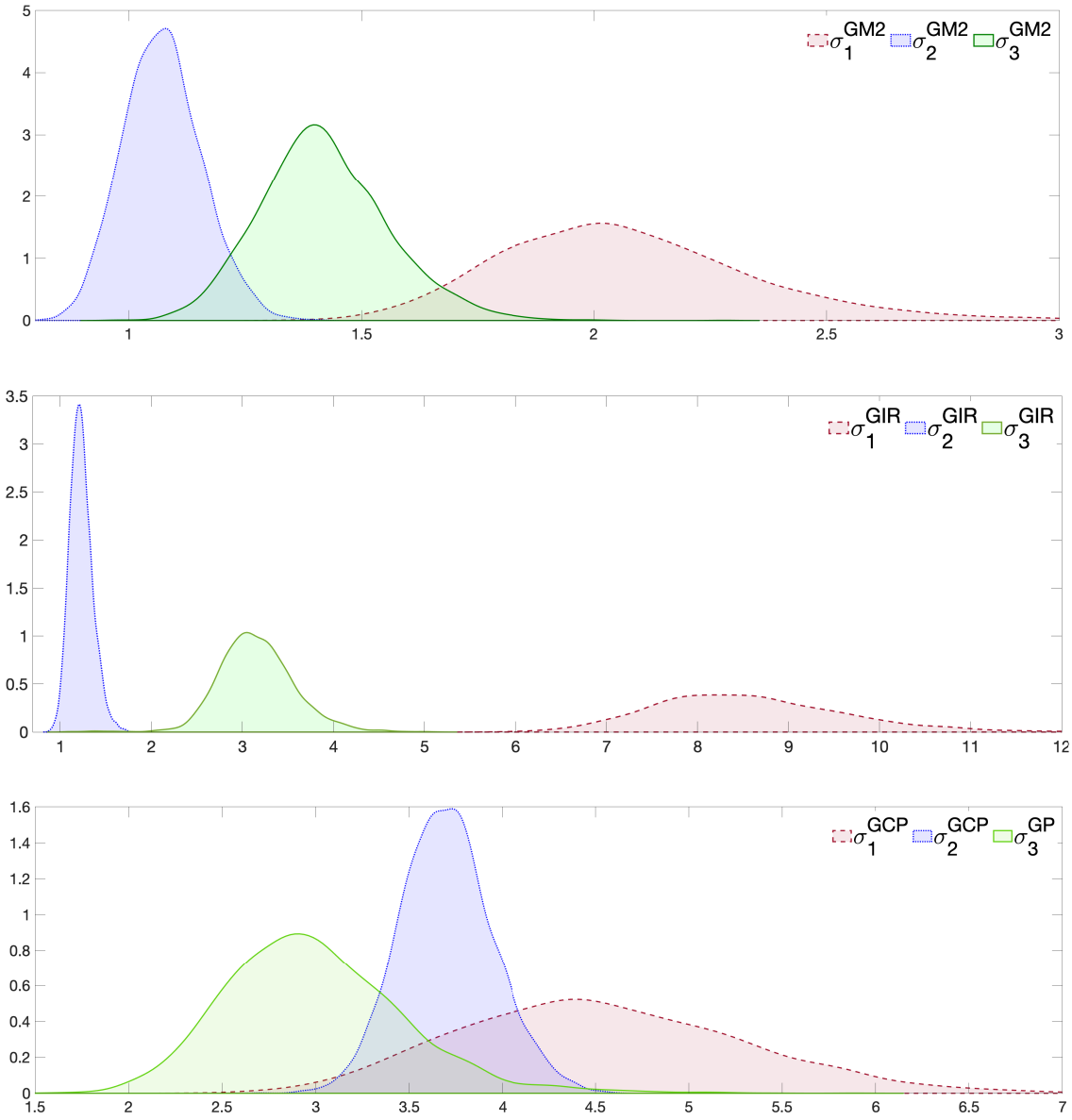

Figure 4: Upper panel: σ_1^{GM2}, σ_2^{GM2}, and σ_3^{GM2} are respectively kernel density estimates of the posterior draws of the regime-dependent standard deviation of global money supply in the first (red shaded area with dashed line), second (blue shaded area with dotted line), and third (green shaded area with continuous line) regimes. Middle panel: σ_1^{GIR}, σ_2^{GIR}, and σ_3^{GIR} are respectively kernel density estimates of the posterior draws of the regime-dependent standard deviation of global interest rate in the first (red shaded area with dashed line), second (blue shaded area with dotted line), and third (green shaded area with continuous line) regimes. Lower panel: σ_1^{GCP}, σ_2^{GCP}, and σ_3^{GCP} are respectively kernel density estimates of the posterior draws of the regime-dependent standard deviation of commodity price in the first (red shaded area with dashed line), second (blue shaded area with dotted line), and third (green shaded area with continuous line) regimes.

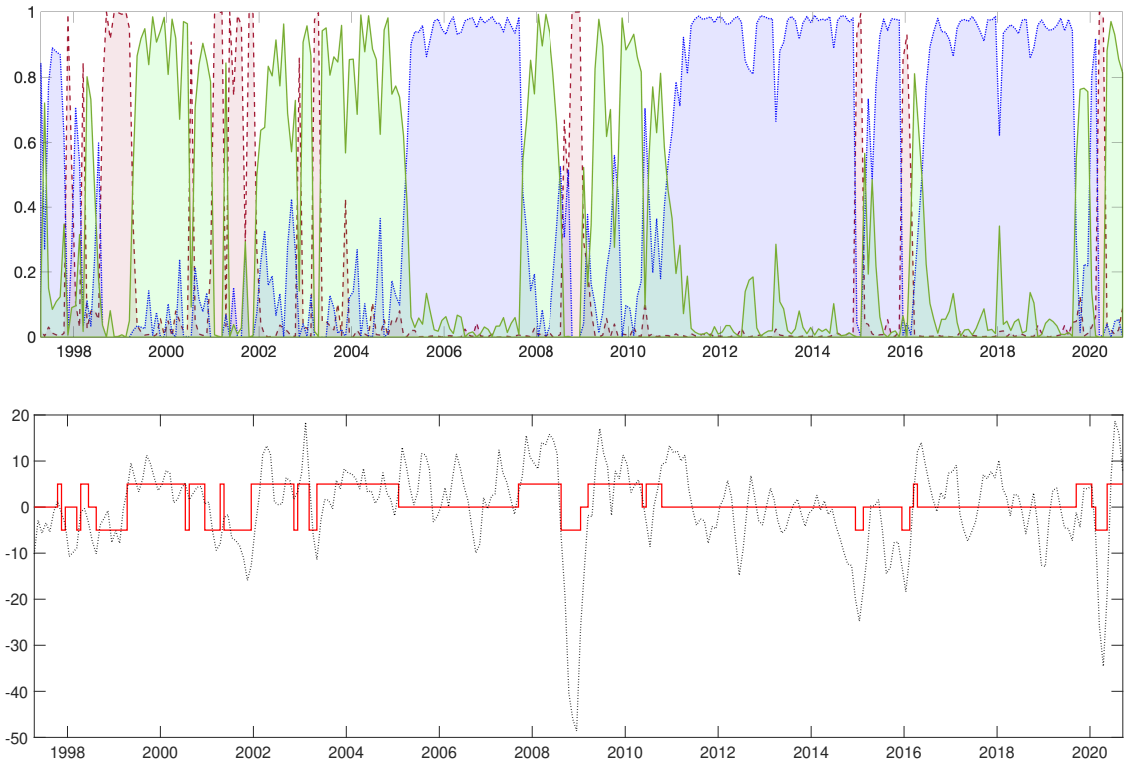

Figure 5: Upper panel: The red shaded area with dashed line refers to the filtered probability of regime 1, the blue shaded area with dotted line is the filtered probability of regime 2, and the green shaded area with continuous line is the filtered probability of regime 3. Lower panel: It shows the growth of commodity prices (black dotted line) and the filtered state (red line). When the red line is 0 indicates evidence of the second regime, when it is equal to -5 indicates evidence of the first regime, and when it is 5, it indicates evidence of the third regime.

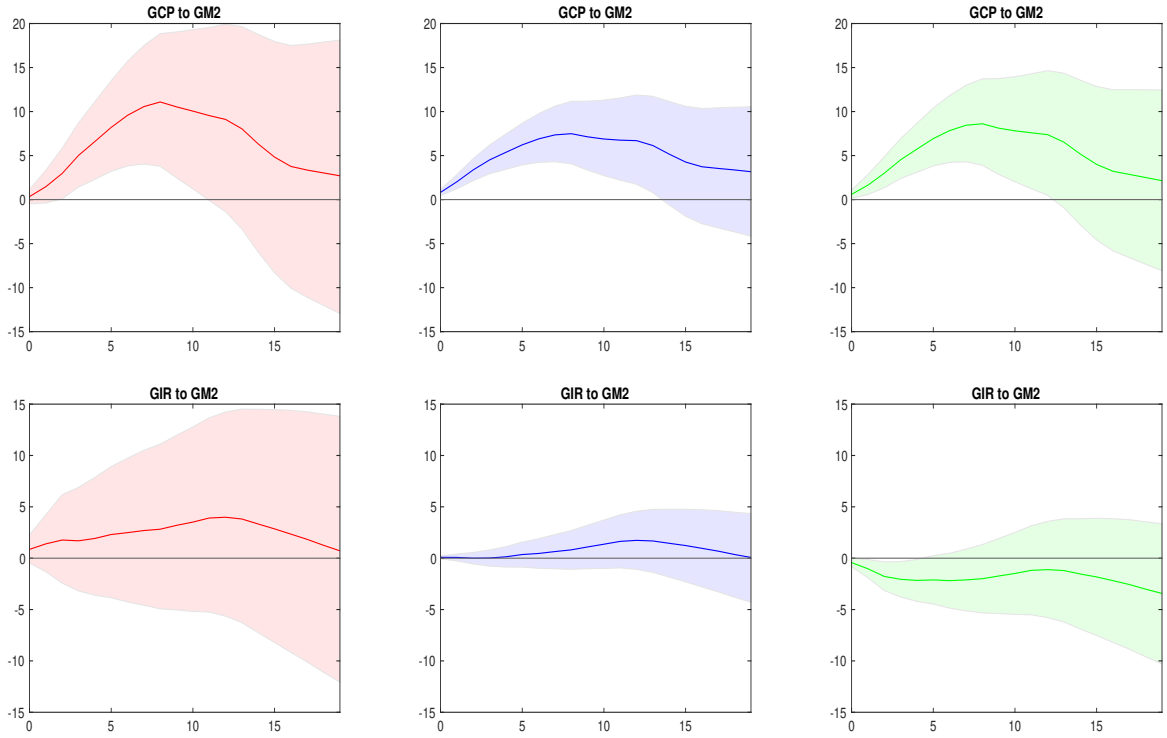

Figure 6: The first and the second rows represent the impulse response functions (IRFs) of commodity prices (GCP) and global interest rates (GIR) to global money supply (GM2) shock, respectively. Each column reports the IRFs in a specific regime. Particularly, on the left are the IRFs in the first regime, on the right are the IRFs in the third regime, and in the middle are the IRFs in the second regime. The solid lines are the median responses, whereas the shaded areas correspond to 68% credible intervals.

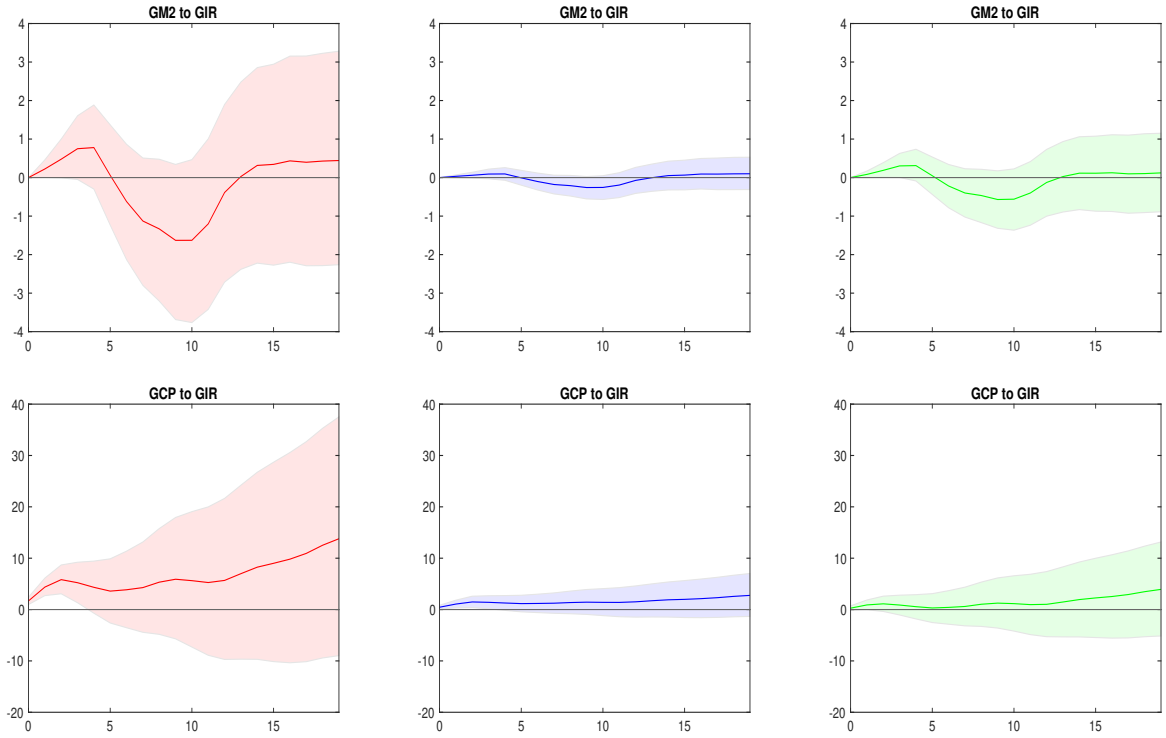

Figure 7: The first and the second rows represent the impulse response functions (IRFs) of global money supply (GM2) and commodity prices (GCP) to a global interest rate (GIR) shock, respectively. Each column reports the IRFs in a specific regime. Particularly, on the left are the IRFs in the first regime, on the right are the IRFs in the third regime, and in the middle are the IRFs in the second regime. The solid lines are the median responses, whereas the shaded areas correspond to 68% credible intervals.

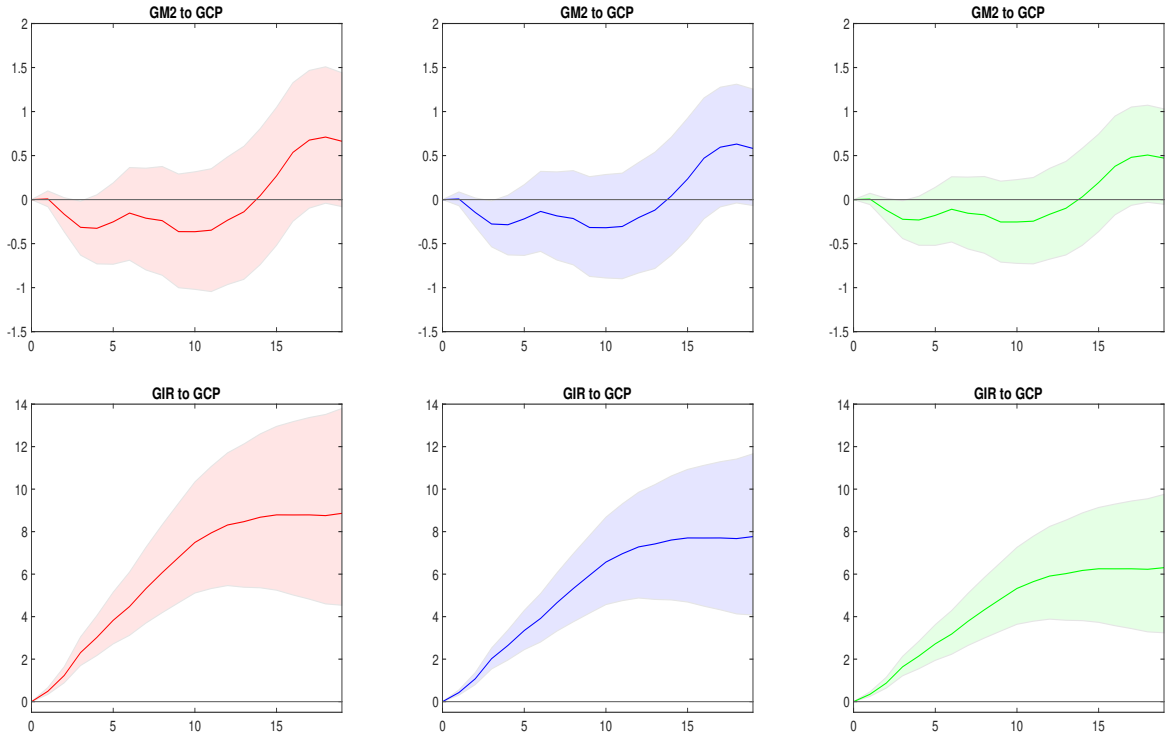

Figure 8: The first and the second rows represent the impulse response functions (IRFs) of global money supply (GM2) and global interest rate (GIR) to a commodity price (GCP) shock, respectively. Each column reports the IRFs in a specific regime. Particularly, on the left are the IRFs in the first regime, on the right are the IRFs in the third regime, and in the middle are the IRFs in the second regime. The solid lines are the median responses, whereas the shaded areas correspond to 68% credible intervals.

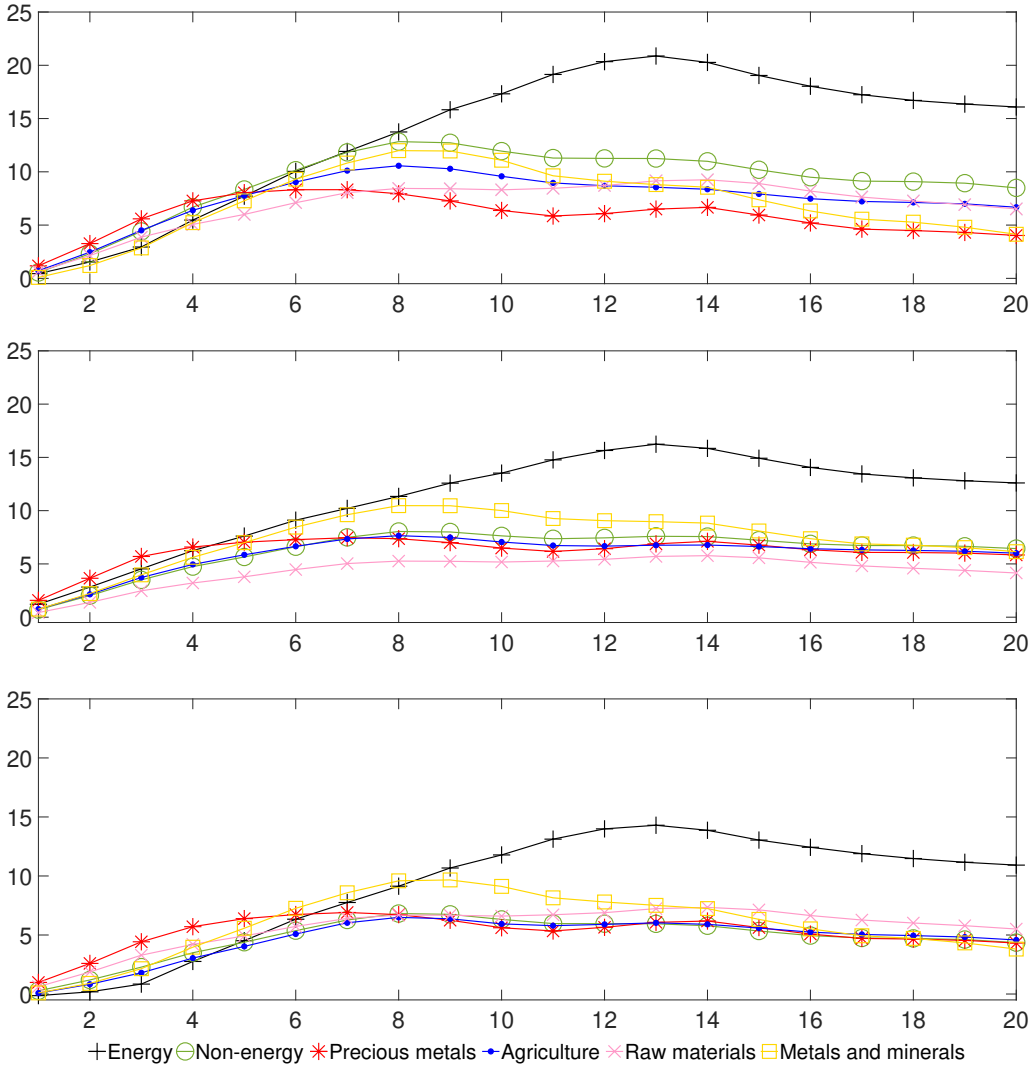

Figure 9: Upper panel: Cumulated impulse response functions of energy, non-energy, precious metals, agriculture, raw materials, and metals and minerals to a global money supply shock in the first regime. Middle panel: Cumulated impulse response functions of energy, non-energy, precious metals, agriculture, raw materials, and metals and minerals to a global money supply shock in the second regime. Lower panel: Cumulated impulse response functions of energy, non-energy, precious metals, agriculture, raw materials, and metals and minerals to a global money supply shock in the third regime.

APPENDIX

A Priors

This Appendix shows the priors that we use to estimate the MS-VAR model.

Prior specification for regime-independent parameters: The prior distribution of regime-independent autoregressive coefficients, $\boldsymbol{\gamma}_0$, is:

$$\boldsymbol{\gamma}_0 \sim \mathcal{N}_{K^2P}(\underline{\boldsymbol{\gamma}}_0, \underline{\boldsymbol{\Sigma}}_0), \tag{13}$$

where $\underline{\boldsymbol{\gamma}}_0 = \mathbf{0}_{K^2P}$, a $K^2P \times 1$ null vector, and $\underline{\boldsymbol{\Sigma}}_0 = 10\mathbf{I}_{K^2P}$.

Prior specification for the regime-dependent intercepts: The prior distribution of the MS intercepts, $\boldsymbol{\gamma}_i$, is:

$$\boldsymbol{\gamma}_i \sim \mathcal{N}_K(\underline{\boldsymbol{\gamma}}_i, \underline{\boldsymbol{\Sigma}}_i), \quad \text{for} \quad i = 1, \ldots, M, \tag{14}$$

where $\underline{\boldsymbol{\gamma}}_i = \mathbf{0}_K$, a $K \times 1$ null vector, and $\underline{\boldsymbol{\Sigma}}_i = 10\mathbf{I}_K$.

Prior specification for the regime dependent variance-covariance matrices: The prior chosen for the inverse of the regime-specific variance-covariance matrices is independent Wishart ($\mathcal{W}$) priors, which read as:

$$\boldsymbol{\Sigma}_i^{-1} \sim \mathcal{W}_K(\underline{\boldsymbol{\Upsilon}}_i, \underline{\nu}_i) \quad \text{for} \quad i = 1, \ldots, M \tag{15}$$

where $\underline{\nu}_i = 5$ is the degrees of freedom parameter and $\underline{\Upsilon}_i = 10\mathbf{I}_K$ is the scale matrix.

Prior specification for the parameters of the time-varying transition probabilities matrix: In order to void overfitting, following Billio et al. (2016), we use a hierarchical prior specification for the parameters of the Logit specification in time-varying transition probabilities. Specifically, for the parameters which drive the j-th row in the

matrix in Equation (2), we assume:

$$\begin{aligned} \boldsymbol{\theta}^{ij} &\sim \mathcal{N}_{N+1}\left(\boldsymbol{\psi}, \boldsymbol{\Omega}\right) \quad i = 1, \ldots, M-1 \\ \boldsymbol{\psi} &\sim \mathcal{N}_{N+1}(\underline{\boldsymbol{\psi}}, \underline{\boldsymbol{\Omega}}) \end{aligned} \tag{16}$$

with $\underline{\boldsymbol{\psi}} = \mathbf{0}_N$, a $N \times 1$ null vector, $\boldsymbol{\Omega} = \mathbf{I}_{N+1}$ and $\underline{\boldsymbol{\Omega}} = 10\mathbf{I}_{N+1}$.

B Posteriors

Posterior of the regime-independent parameters: The posterior distribution of the regime-independent parameter, $\boldsymbol{\gamma}_0$, is normal with density function:

$$\begin{aligned} &f\left(\boldsymbol{\gamma}_0 \mid \mathbf{y}, \boldsymbol{\Xi}, \boldsymbol{\gamma}, \boldsymbol{\Sigma}, \underline{\boldsymbol{\gamma}_0}\right) \propto \\ &\propto \exp\left\{-\frac{1}{2}\boldsymbol{\gamma}_0'\left(\sum_{t=1}^{T}\mathbf{X}_{0t}'\boldsymbol{\Sigma}_t^{-1}\mathbf{X}_{0t} + \underline{\boldsymbol{\Sigma}}_0^{-1}\right)\boldsymbol{\gamma}_0 + \boldsymbol{\gamma}_0\left(\sum_{t=1}^{T}X_{0t}'\boldsymbol{\Sigma}_t^{-1}\mathbf{y}_{0t} + \underline{\boldsymbol{\Sigma}}_0^{-1}\underline{\boldsymbol{\gamma}}_0\right)\right\} \\ &\propto \mathcal{N}_{K^2P}\left(\bar{\boldsymbol{\gamma}}_0, \bar{\boldsymbol{\Sigma}}_0\right), \end{aligned} \tag{17}$$

where $\mathbf{y}_{0t} = \mathbf{y}_t - \sum_{i=1}^{M}\xi_{it}\mathbf{X}_{it}\boldsymbol{\gamma}_i$, $\bar{\boldsymbol{\gamma}}_0 = \bar{\boldsymbol{\Sigma}}_0\left(\underline{\boldsymbol{\Sigma}}_0^{-1}\underline{\boldsymbol{\gamma}}_0 + \sum_{t=1}^{T}\mathbf{X}_{0t}'\boldsymbol{\Sigma}_t^{-1}\mathbf{X}_{0t}\right)$, and $\bar{\boldsymbol{\Sigma}}_0^{-1} = (\underline{\boldsymbol{\Sigma}}_0^{-1} + \sum_{t=1}^{T}\mathbf{X}_{0t}'\boldsymbol{\Sigma}_t^{-1}\mathbf{X}_{0t})$

Posterior of the regime dependent intercepts: The conditional posterior distributions of $\boldsymbol{\gamma}_i$, with $i = 1, \ldots, M$, are normal with density functions:

$$\begin{aligned} &f\left(\boldsymbol{\gamma}_i \mid \mathbf{y}, \boldsymbol{\Xi}, \boldsymbol{\gamma}_0, \boldsymbol{\gamma}_{(-i)}, \boldsymbol{\Sigma}, \underline{\boldsymbol{\gamma}_i}\right) \propto \\ &\propto \exp\left\{-\frac{1}{2}\boldsymbol{\gamma}_i'\left(\sum_{t\in\mathcal{T}_i}\mathbf{X}_{it}'\boldsymbol{\Sigma}_t^{-1}\mathbf{X}_{it} + \underline{\boldsymbol{\Sigma}}_i^{-1}\right)\boldsymbol{\gamma}_i + \boldsymbol{\gamma}_i'\left(\sum_{t\in\mathcal{T}_i}\mathbf{X}_{it}'\boldsymbol{\Sigma}_t^{-1}\mathbf{y}_{it} + \underline{\boldsymbol{\Sigma}}_i^{-1}\underline{\boldsymbol{\gamma}}_i\right)\right\} \\ &\propto \mathcal{N}_K\left(\bar{\boldsymbol{\gamma}}_i, \bar{\boldsymbol{\Sigma}}_i\right) \end{aligned} \tag{18}$$

with $\overline{\boldsymbol{\gamma}}_i = \bar{\boldsymbol{\Sigma}}_i^{-1}\left(\underline{\boldsymbol{\Sigma}}_i^{-1}\underline{\boldsymbol{\gamma}}_i + \sum_{t\in\mathcal{T}_i}\mathbf{X}_{it}'\boldsymbol{\Sigma}_t^{-1}\mathbf{X}_{it}\right)$ and $\bar{\boldsymbol{\Sigma}}_i^{-1} = \left(\underline{\boldsymbol{\Sigma}}_i^{-1} + \sum_{t\in\mathcal{T}_i}\mathbf{X}_{it}'\boldsymbol{\Sigma}_t^{-1}\mathbf{X}_{it}\right)$ where $\mathcal{T}_i = \{t \mid \xi_{it} = 1, t = 1, \ldots, T\}$ and $\mathbf{y}_{it} = \mathbf{y}_t - \mathbf{X}_{0t}\boldsymbol{\gamma}_0$.

Posterior of the regime dependent variance-covariance matrices: The conditional posterior distribution of the regime-dependent variance-covariance matrix, $\boldsymbol{\Sigma}_i$, with $i = 1, \ldots, M$, are Wishart density:

$$
\begin{aligned}
& f(\boldsymbol{\Sigma}_i^{-1} \mid \mathbf{y}, \boldsymbol{\Xi}, \boldsymbol{\gamma}_0, \boldsymbol{\gamma}_i, \boldsymbol{\Sigma}_{(-i)}, \underline{\boldsymbol{\Upsilon}}_i) \propto \\
& \propto \mid \boldsymbol{\Sigma}_i^{-1} \mid^{\frac{\nu_i + T_i - K - 1}{2}} \exp\left\{ -\frac{1}{2} \mathrm{tr}\left(\left(\underline{\boldsymbol{\Upsilon}}_i^{-1} + \sum_{t \in \mathcal{T}_i} \mathbf{u}_{it} \mathbf{u}_{it}' \right) \boldsymbol{\Sigma}_i^{-1} \right) \right\} \\
& \propto \mathcal{W}_K(\bar{\nu}_i, \bar{\boldsymbol{\Upsilon}}_i)
\end{aligned}
\tag{19}
$$

where $T_i = \sum_{t=1}^{T} \mathbb{I}_{\xi_{it}=1}$, $\mathbf{u}_{it} = \mathbf{y}_t - \mathbf{X}_{0t}\boldsymbol{\gamma}_0 - X_{it}\boldsymbol{\gamma}_i$, $\bar{\nu}_i = \underline{\nu}_i + T_i$, and $\bar{\boldsymbol{\Upsilon}}_i = \underline{\boldsymbol{\Upsilon}}_i + \sum_{t \in \mathcal{T}_i} \mathbf{u}_{it}\mathbf{u}_{it}'$.

Posterior of the parameters of the time-varying transition probabilities matrix: The full conditional distribution of the parameters in the j-th row of the transition matrix is:

$$
f\left(\boldsymbol{\theta}^{j1}, \ldots, \boldsymbol{\theta}^{j(M-1)} | \mathbf{y}, \boldsymbol{\Xi}, \boldsymbol{\gamma}_i \right) \propto \prod_{t=1}^{T} \prod_{i=1}^{M-1} \left(G\left(\mathbf{V}_t, \boldsymbol{\theta}^{ki} \right) \right)^{\xi_{it}\xi_{jt-1}}, \tag{20}
$$

and we apply a Metropolis-Hastings.

C IRFs of commodity sectors

First regime												
Horizon	4			8			12			16		
	LB	Median	UB	LB	Median	UB	LB	Median	UB	LB	Median	UB
Energy	-0.8	5.5	11.9	2.6	13.7	25.1	4.5	20.3	36.4	-2.5	18.0	38.7
Non-Energy	3.4	6.7	10.1	6.9	12.8	19.1	2.5	11.3	20.3	-2.1	9.5	21.2
Precious metals	4.6	7.3	10.1	2.6	7.9	13.6	-2.1	6.1	14.5	-5.8	5.2	16.3
Agriculture	4.0	6.4	9.1	6.1	10.6	15.6	2.0	8.7	15.9	-1.5	7.5	16.8
Raw Materials	3.3	5.1	7.0	5.1	8.4	12.2	3.5	8.7	14.2	1.3	8.2	15.5
Metals and minerals	1.4	5.2	9.1	4.4	12.0	19.9	-2.3	9.1	21.0	-8.8	6.3	21.7
Second regime												
Horizon	4			8			12			16		
	LB	Median	UB	LB	Median	UB	LB	Median	UB	LB	Median	UB
Energy	3.2	6.2	9.4	5.3	11.3	17.5	6.7	15.6	24.7	2.3	14.1	26.0
Non-Energy	3.6	4.7	5.9	5.8	8.0	10.3	4.0	7.4	10.9	2.2	6.9	11.6
Precious metals	4.4	6.6	8.4	3.6	7.4	10.7	1.2	6.4	11.3	-0.4	6.3	12.8
Agriculture	3.8	4.9	6.1	5.4	7.7	10.0	3.2	6.7	10.2	1.8	6.4	11.1
Raw Materials	2.1	3.2	4.3	3.2	5.3	7.4	2.3	5.4	8.6	1.0	5.1	9.3
Metals and minerals	3.6	5.6	7.8	6.4	10.5	14.8	2.8	9.1	15.7	-5.7	7.4	16.0
Third regime												
Horizon	4			8			12			16		
	LB	Median	UB	LB	Median	UB	LB	Median	UB	LB	Median	UB
Energy	-0.7	2.8	6.7	2.0	9.1	17.2	3.5	14.0	25.8	-1.6	12.4	27.7
Non-Energy	2.3	3.5	4.7	4.4	6.8	9.6	2.2	6.0	9.9	-0.2	4.9	10.2
Precious metals	2.9	5.7	8.9	2.0	6.7	11.9	-1.3	5.6	12.9	-3.9	5.1	14.4
Agriculture	1.2	3.0	5.3	3.0	6.5	10.7	0.8	5.9	11.9	-1.5	5.2	13.0
Raw Materials	1.6	4.2	7.0	2.8	6.7	11.0	1.7	6.9	12.5	0.1	6.6	13.6
Metals and minerals	1.5	4.0	6.7	4.3	9.6	15.5	-0.7	7.8	16.6	-5.9	5.5	16.9

Table 4: This table shows values of median impulse response functions, together with respective 68% confidence bandwidths in each regime; LB stands for the lower bound, while UB stands for the upper bound.